PERGAMON

Mechatronics 12 (2002) 357–370

MECHATRONICS

Inverted pendulum systems: rotary and arm-driven - a mechatronic system design case study

S. Awtar, N. King, T. Allen, I. Bang, M. Hagan, D. Skidmore, K. Craig *

Department of Mechanical Engineering, Aeronautical Engineering and Mechanics, Rensselaer Polytechnic Institute, Troy, NY 12180, USA

Abstract

The inverted pendulum, a popular mechatronic application, exists in many different forms. The common thread among these systems is to balance a link on end using feedback control. Two challenging inverted pendulum systems are the rotational and arm-driven systems. The system described in this paper can be transformed from the rotational to the arm-driven configuration by replacing the links and setting the base on its side. It was designed and built by students as part of the course *Mechatronic System Design* at Rensselaer. This paper presents a summary of a mechatronic system design case study for the rotary inverted pendulum system.

1. Introduction: Mechatronics at Rensselaer

Mechatronics is the *synergistic* combination of mechanical engineering, electronics, control systems, and computers. The key element in mechatronics is the *integration* of these areas through the design process. The essential characteristic of a mechatronics engineer and the key to success in mechatronics is a *balance* between two sets of skills: modeling/analysis skills and experimentation/hardware implementation skills. *Synergism* and *integration* in design set a *mechatronic system* apart from a traditional, multidisciplinary system. Mechanical engineers are expected to

* Corresponding author.
E-mail address: craigk@rpi.edu (K. Craig).

0957-4158/02/$ - see front matter
PII: S0957-4158(01)00075-7

design with synergy and integration and professors must now teach design accordingly.

Rensselaer – the nation's first technological university – was founded in 1824. A nonsectarian, coeducational, private university, it is home to five schools – Architecture, Engineering, Humanities and Social Sciences, Lally School of Management and Technology, and Science – as well as the interdisciplinary faculty of Information Technology. Rensselaer enrolls more than 9600 undergraduates, graduate students, and working professionals at campuses in Troy, NY, and Hartford, CT, and through distance learning opportunities around the world. With 2600 students, Rensselaer's School of Engineering offers one of the largest undergraduate engineering programs of any private university in the country. In recent years Rensselaer has been consistently ranked among the top 20 engineering teaching and research universities in the US.

Undergraduate engineering education at Rensselaer consists of two phases: an interdisciplinary core curriculum during the first two years, with instruction from various departments, followed by the disciplinary curriculum implemented by an individual department. The Department of Mechanical Engineering, Aeronautical Engineering, and Mechanics at Rensselaer offers bachelor, master, and doctoral degrees in the three disciplines represented in the name. The department awards over 200 bachelor, 80 master, and 20 doctoral degrees per year, the major portion of which are mechanical engineering degrees. In the department there are presently two senior-elective courses in the field of mechatronics, which are also open to graduate students: *Mechatronics*, offered in the fall semester, and *Mechatronic System Design*, offered in the spring semester. In both courses, emphasis is placed on a balance between physical understanding and mathematical formalities. The key areas of study covered in both courses are:

1. mechatronic system design principles;
2. modeling, analysis, and control of dynamic physical systems;
3. selection and interfacing of sensors, actuators, and microcontrollers;
4. analog and digital control electronics;
5. real-time programming for control.

Mechatronics covers the fundamentals in these areas through integrated lectures and laboratory exercises, while *Mechatronic System Design* focuses on the application and extension of the fundamentals through a design, build, and test experience. Throughout the coverage, the focus is kept on the role of the key mechatronic areas of study in the overall design process and how these key areas are integrated into a successful mechatronic system design.

In mechatronics, balance is paramount. The essential characteristic of a mechatronics engineer and the key to success in mechatronics is a balance between two skill sets:

1. Modeling (physical and mathematical), analysis (closed-form and numerical simulation), and control design (analog and digital) of dynamic physical systems.
2. Experimental validation of models and analysis (for computer simulation without experimental verification is at best questionable, and at worst useless), and an understanding of the key issues in hardware implementation of designs.

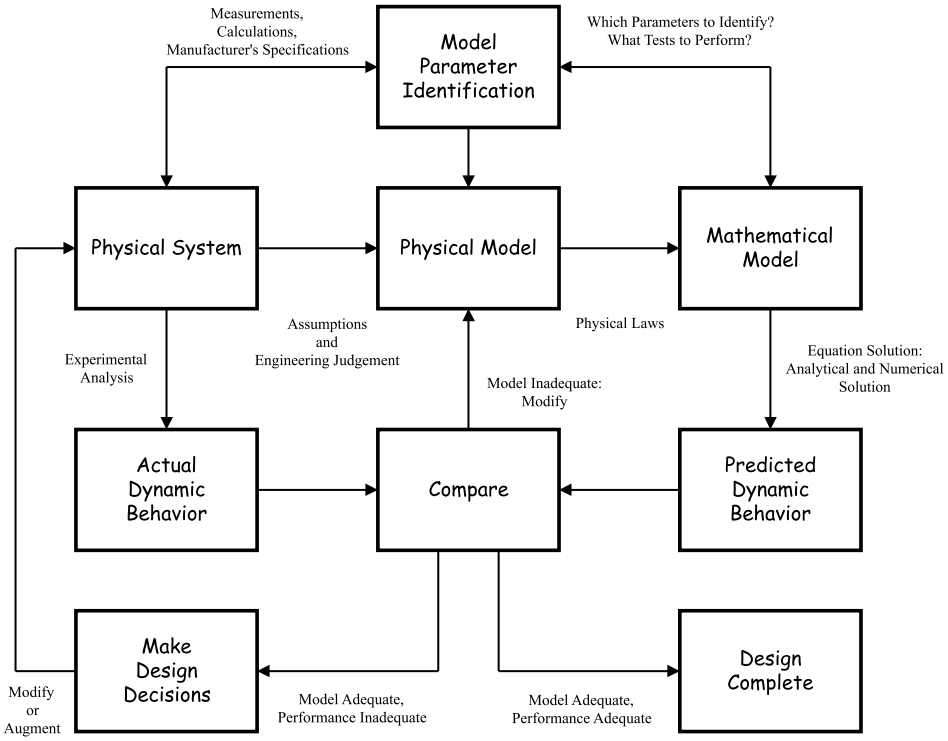

Fig. 1. Dynamic system investigation process.

Fig. 1 shows a diagram of the procedure for a *dynamic system investigation* which emphasizes this balance. Here the physical system can be an actual device or system that one needs to understand and possibly improve, or it can represent a concept being evaluated in the design process. Engineers can no longer evaluate each design concept by building and testing; it is too costly and time consuming. They must rely on modeling and analysis and previous hardware experience to evaluate each design concept with the goal of building choice prototypes only.

This diagram serves as a guide for the study of the various mechatronic hardware systems in the courses taught at Rensselaer. When students perform a complete dynamic system investigation of a mechatronic system, they develop modeling/analysis skills and obtain knowledge of and experience with a wide variety of analog and digital sensors and actuators that will be indispensable as mechatronic design engineers in future years.

2. Inverted pendulum system: rotary and arm-driven

The inverted pendulum is a popular mechatronic application that exists in many different forms. The common thread among these systems is their goal: to balance a

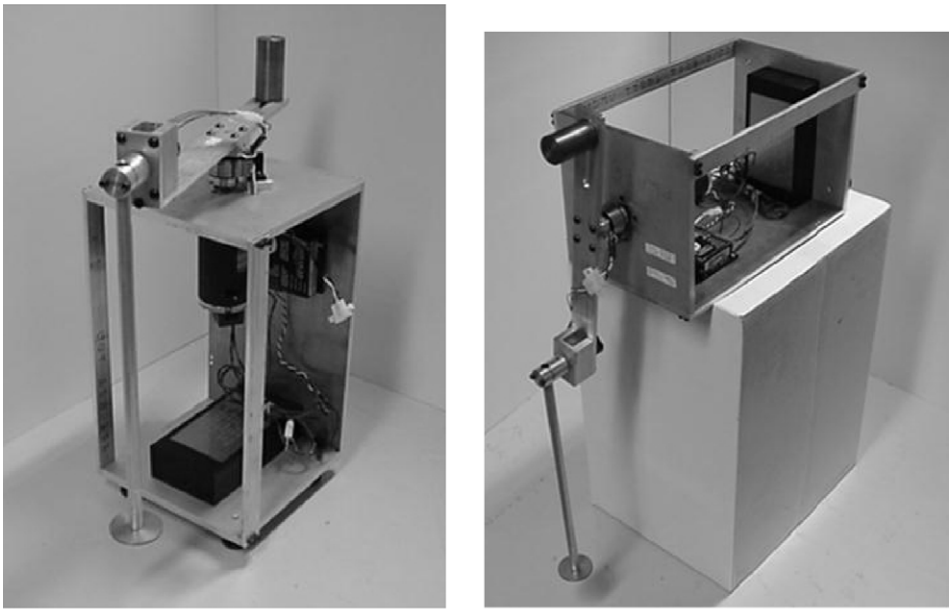

Fig. 2. Inverted pendulum system configurations: (a) horizontal and (b) vertical.

link on end using feedback control. Two rather challenging inverted pendulum systems are the rotational and the arm-driven systems. These use a link rotating about an axis to balance a second link on end. In the rotary (horizontal) configuration, the first link, driven by a motor, rotates in the horizontal plane to balance a pendulum link, which rotates freely in the vertical plane. The arm-driven (vertical) or ''stick-on-a-stick'' configuration uses a driven link rotating in the vertical plane to balance the pendulum link, which also rotates in the vertical plane. The inverted pendulum system is unique in that it can be transformed from the horizontal to vertical configuration by replacing the links and setting the base on its side, as shown in Fig. 2.

The complete mechatronic system design includes design concept generation, mechanical/electromechanical dynamic analysis, simulation of system dynamics, component selection and fabrication, electronic hardware and transducer selection and interfacing, circuit design and wiring, software design, system parameter identification and verification, and finally, controller design, swing-up and balance, and implementation.

3. Rotary inverted pendulum dynamic system investigation

In this section, highlights of the complete dynamic system investigation are presented.

3.1. Physical system

The subject of this investigation is the rotary inverted pendulum system. It consists of two links: a motor-driven horizontal link and an un-actuated vertical pendulum link. The horizontal link is driven by a permanent-magnet, brushed DC motor. A DC power supply together with a pulse-width-modulated (PWM) servo-amplifier, operating in the current mode, supplies power to the motor. Angular position and velocity of the two links are measured with two rotary incremental optical encoders having a resolution with quadrature decoding of 2048 pulses per revolution. A slip-ring assembly, mounted between the housing and the motor shaft, is used to connect power to the pendulum optical encoder and read the signal from the three channels of the encoder. The horizontal link is counter-weighted and there are leveling screws on the housing base.

System testing for parameter identification and control system design is performed in a MatLab/Simulink/dSpace real-time control environment. This allows for rapid control system development and testing.

3.2. Physical model

Several simplifying assumptions were made in developing a physical model:

1. Rigid links.
2. Two degrees of freedom.
3. Assume both Coulomb and viscous friction, in the motor, in the slip-ring assembly, and at the pendulum revolute joint, for initial control design.
4. Dynamic response of the encoders is sufficiently fast that it can be considered instantaneous.
5. Dynamic response of the servo-amplifier is sufficiently fast that it can be considered instantaneous.
6. Motor operates in the torque mode with $V_{\text{in}}K_{\text{A}} = i$ and $T = K_{\text{T}}i$, where
   K_{T} is the motor torque constant (N m/A),
   K_{A} is the amplifier constant (A/V),
   V_{in} is the command voltage (V),
   T is the electromagnetic torque applied to the motor rotor (N m),
   i is the motor current (A).
7. Motor is modeled in a lumped-parameter way, where
   J is the rotor inertia (N m s^2/rad = kg m^2),
   B_{f} is the viscous friction coefficient (N m s/rad),
   T_{f} is the Coulomb friction torque (N m).
8. Body-fixed axes are principal axes for link 2, the pendulum link (This assumption needs to be verified experimentally.).

Fig. 3 shows the physical model geometry.

The absolute angular velocities of the two links are given by

$$\begin{aligned} {}^{R}\vec{\omega}^{R_1} &= \dot{\theta}\hat{k}, \\ {}^{R}\vec{\omega}^{R_2} &= \dot{\phi}\cos\theta\hat{i} + \dot{\phi}\sin\theta\hat{j} + \dot{\theta}\hat{k}. \end{aligned} \tag{1}$$

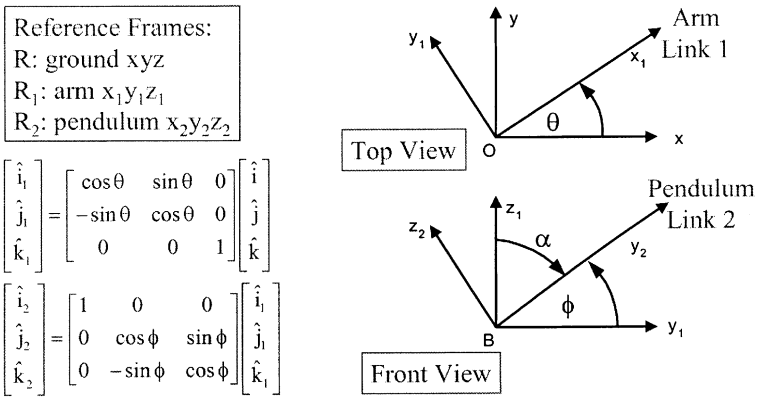

Fig. 3. Physical model geometry.

The absolute velocities of the CG's of the two links (point A for link 1, point C for link 2) are given by

$$
\begin{aligned}
{}^{R}\vec{V}^{A} &= (-\ell_{11}\dot{\theta}\sin\theta)\hat{i} + (\ell_{11}\dot{\theta}\cos\theta)\hat{j},\\
{}^{R}\vec{V}^{C} &= (-\dot{\theta}\ell_1\sin\theta - \dot{\theta}\ell_{21}\cos\phi\cos\theta + \dot{\phi}\ell_{21}\sin\phi\sin\theta)\hat{i}\\
&\quad + (\dot{\theta}\ell_1\cos\theta - \dot{\theta}\ell_{21}\cos\phi\sin\theta - \dot{\phi}\ell_{21}\sin\phi\cos\theta)\hat{j} + (\dot{\phi}\ell_{21}\cos\phi)\hat{k},
\end{aligned}
\tag{2}
$$

where

$$
\begin{aligned}
\ell_1 &= \text{length of link 1} = \ell_{11} + \ell_{12},\\
\ell_{11} &= \text{distance from pivot O to CG of link 1},\\
\ell_{12} &= \text{distance from CG of link 1 to end of link 1},
\end{aligned}
\tag{3}
$$

$$
\begin{aligned}
\ell_2 &= \text{length of link 2} = \ell_{21} + \ell_{22},\\
\ell_{21} &= \text{distance from pivot B to CG of link 2},\\
\ell_{22} &= \text{distance from CG of link 2 to end of link 2}.
\end{aligned}
\tag{4}
$$

3.3. Mathematical model

The Lagrange method was used to derive the equations of motion for the system. The generalized coordinates for the system are the angular displacements of the driven link (θ) and the pendulum link (ϕ). Lagrange's equations are given by

$$
\frac{\mathrm{d}}{\mathrm{d}t}\left(\frac{\partial T}{\partial \dot{q}_i}\right) - \frac{\partial T}{\partial q_i} + \frac{\partial V}{\partial q_i} = Q_i \tag{5}
$$

with generalized coordinates

$$
\begin{aligned}
q_1 &= \theta,\\
q_2 &= \phi.
\end{aligned}
\tag{6}
$$

The expressions for the potential energy, V, and kinetic energy, T, for the system are given by

$$V = -m_2 g \ell_{21}(1 - \sin\phi), \tag{7}$$

$$T = \frac{1}{2} m_1 \left({}^R V^A\right)^2 + \frac{1}{2} \bar{I}_{1_{z_1}} \dot{\theta}^2 + \frac{1}{2} m_2 \left({}^R V^C\right)^2 + \frac{1}{2}\left[\bar{I}_{2_{x_2}} \dot{\phi}^2 + \bar{I}_{2_{y_2}} (\sin^2\phi)\dot{\theta}^2 + \bar{I}_{2_{z_2}} (\cos^2\phi)\dot{\theta}^2\right]. \tag{8}$$

The generalized torques for the Lagrange formulation are given by

$$\begin{aligned} Q_\theta &= T - B_\theta \dot{\theta} - T_{f\theta} \mathrm{sgn}(\dot{\theta}) \\ Q_\phi &= -B_\phi \dot{\phi} - T_{f\phi} \mathrm{sgn}(\dot{\phi}) \end{aligned} \tag{9}$$

where

$T =$ motor torque,
$B_\theta =$ viscous damping constant θ joint,
$T_{f\theta} =$ Coulomb friction constant θ joint,
$B_\phi =$ viscous damping constant ϕ joint,
$T_{f\phi} =$ Coulmob friction constant ϕ joint.

Applying the Lagrange formulation to the system with the two generalized coordinates θ and ϕ results in

$$\begin{aligned} \frac{\mathrm{d}}{\mathrm{d}t}\frac{\partial T}{\partial \dot{\theta}} - \frac{\partial T}{\partial \theta} + \frac{\partial V}{\partial \theta} &= Q_\theta, \\ \frac{\mathrm{d}}{\mathrm{d}t}\frac{\partial T}{\partial \dot{\phi}} - \frac{\partial T}{\partial \phi} + \frac{\partial V}{\partial \phi} &= Q_\phi, \end{aligned} \tag{10}$$

$$\begin{aligned} &\left[m_1 \ell_{11}^2 + \bar{I}_{1_{z_1}} + m_2 \ell_1^2 + m_2 \ell_{21}^2 \cos^2\phi + \bar{I}_{2_{z_2}} \cos^2\phi + \bar{I}_{2_{y_2}} \sin^2\phi\right]\ddot{\theta} \\ &\quad - [m_2 \ell_1 \ell_{21} \sin\phi]\ddot{\phi} - [m_2 \ell_1 \ell_{21} \cos\phi]\dot{\phi}^2 + \left[\bar{I}_{2_{y_2}} - m_2 \ell_{21}^2 - \bar{I}_{2_{z_2}}\right] \\ &\quad \times (2\cos\phi \sin\phi)\dot{\phi}\dot{\theta} = T - \left[B_\theta \dot{\theta} + T_{f\theta} \mathrm{sgn}(\dot{\theta})\right], \end{aligned} \tag{11}$$

$$\begin{aligned} &\left[m_2 \ell_{21}^2 + \bar{I}_{2_{x_2}}\right]\ddot{\phi} - [m_2 \ell_1 \ell_{21} \sin\phi]\ddot{\theta} + \left[m_2 \ell_{21}^2 - \bar{I}_{2_{y_2}} + \bar{I}_{2_{z_2}}\right](\cos\phi \sin\phi)\dot{\theta}^2 \\ &\quad + m_2 g \ell_{21} \cos\phi = -\left[B_\phi \dot{\phi} + T_{f\phi} \mathrm{sgn}(\dot{\phi})\right]. \end{aligned} \tag{12}$$

Define

$$\alpha = \frac{\pi}{2} - \phi. \tag{13}$$

When the pendulum is balanced and the driven link is centered, both θ and α are zero. The nonlinear equations of motion are

$$\begin{aligned} &\left[m_1 \ell_{11}^2 + \bar{I}_{1_{z_1}} + m_2 \ell_1^2 + m_2 \ell_{21}^2 \sin^2\alpha + \bar{I}_{2_{z_2}} \sin^2\alpha + \bar{I}_{2_{y_2}} \cos^2\alpha\right]\ddot{\theta} \\ &\quad + [m_2 \ell_1 \ell_{21} \cos\alpha]\ddot{\alpha} + [m_2 \ell_1 \ell_{21} \sin\alpha]\dot{\alpha}^2 + \left[\bar{I}_{2_{z_2}} + m_2 \ell_{21}^2 - \bar{I}_{2_{y_2}}\right] \\ &\quad - (2\cos\alpha \sin\alpha)\dot{\alpha}\dot{\theta} = T - \left[B_\theta \dot{\theta} + T_{f\theta} \mathrm{sgn}(\dot{\theta})\right], \end{aligned} \tag{14}$$

$$-\left[m_2\ell_{21}^2+\bar{I}_{2_{x_2}}\right]\ddot{\alpha}-[m_2\ell_1\ell_{21}\cos\alpha]\ddot{\theta}+\left[m_2\ell_{21}^2-\bar{I}_{2_{y_2}}+\bar{I}_{2_{z_2}}\right](\cos\alpha\sin\alpha)\dot{\theta}^2 + m_2g\ell_{21}\sin\alpha=\left[B_\alpha\dot{\alpha}+T_{f\alpha}\mathrm{sgn}(\dot{\alpha})\right]. \tag{15}$$

The linearized equations of motion (about the operating point $\alpha=\theta=0$) are given by

$$\begin{aligned}&\left[m_1\ell_{11}^2+\bar{I}_{1_{z_1}}+m_2\ell_1^2+\bar{I}_{2_{y_2}}\right]\ddot{\theta}+[m_2\ell_1\ell_{21}]\ddot{\alpha}+=T-B_\theta\dot{\theta},\\&-\left[m_2\ell_{21}^2+\bar{I}_{2_{x_2}}\right]\ddot{\alpha}-[m_2\ell_1\ell_{21}]\ddot{\theta}+m_2g\ell_{21}\alpha=B_\alpha\dot{\alpha}.\end{aligned} \tag{16}$$

Define

$$\begin{aligned}C_1&=m_1\ell_{11}^2+\bar{I}_{1_{z_1}}+m_2\ell_1^2+\bar{I}_{2_{y_2}},\\C_2&=m_2\ell_1\ell_{21},\\C_3&=m_2\ell_{21}^2+\bar{I}_{2_{x_2}},\\C_4&=m_2g\ell_{21}.\end{aligned} \tag{17}$$

The linearized equations of motion can then be written as

$$\begin{aligned}&C_1\ddot{\theta}+C_2\ddot{\alpha}+=T-B_\theta\dot{\theta},\\&C_3\ddot{\alpha}+C_2\ddot{\theta}-C_4\alpha=-B_\phi\dot{\alpha}.\end{aligned} \tag{18}$$

The transfer functions (neglecting damping terms) are

$$\begin{aligned}\frac{\theta}{T}&=\frac{C_3s^2-C_4}{s^2[(C_1C_3-C_2^2)s^2-C_1C_4]},\\\frac{\alpha}{T}&=\frac{-C_2s^2}{s^2[(C_1C_3-C_2^2)s^2-C_1C_4]}.\end{aligned} \tag{19}$$

The state-space equations (neglecting damping terms) are

$$q_1=\theta,\quad q_2=\dot{\theta},\quad q_3=\alpha,\quad q_4=\dot{\alpha},$$

$$\begin{bmatrix}\dot{q}_1\\\dot{q}_2\\\dot{q}_3\\\dot{q}_4\end{bmatrix}=\begin{bmatrix}0&1&0&0\\0&0&\dfrac{-C_2C_4}{C_1C_3-C_2^2}&0\\0&0&0&1\\0&0&\dfrac{C_1C_4}{C_1C_3-C_2^2}&0\end{bmatrix}\begin{bmatrix}q_1\\q_2\\q_3\\q_4\end{bmatrix}+\begin{bmatrix}0\\\dfrac{C_3}{C_1C_3-C_2^2}\\0\\\dfrac{-C_2}{C_1C_3-C_2^2}\end{bmatrix}[T]. \tag{20}$$

3.4. Parameter Identification

Several model parameters need to be identified either analytically or experimentally. They are:

motor parameters,
joint friction: Coulomb and viscous,
masses of links 1 and 2,

location of CG's of links 1 and 2,
moment of inertia for link 1: $\bar{I}_{1_{z_1}}$,
inertia matrix for link 2:

$$\begin{bmatrix} \bar{I}_{2_{x_2}} & \bar{I}_{2_{x_2y_2}} & \bar{I}_{2_{x_2z_2}} \\ \bar{I}_{2_{y_2x_2}} & \bar{I}_{2_{y_2}} & \bar{I}_{2_{y_2z_2}} \\ \bar{I}_{2_{z_2x_2}} & \bar{I}_{2_{z_2y_2}} & \bar{I}_{2_{z_2}} \end{bmatrix}.$$

The inertia matrix for link 2 was determined analytically to be

$$\begin{bmatrix} \bar{I}_{2_{x_2}} & \bar{I}_{2_{x_2y_2}} & \bar{I}_{2_{x_2z_2}} \\ \bar{I}_{2_{y_2x_2}} & \bar{I}_{2_{y_2}} & \bar{I}_{2_{y_2z_2}} \\ \bar{I}_{2_{z_2x_2}} & \bar{I}_{2_{z_2y_2}} & \bar{I}_{2_{z_2}} \end{bmatrix} = \begin{bmatrix} 3.5374\text{E}-3 & -6.5383\text{E}-5 & 0 \\ -6.5383\text{E}-5 & 2.8457\text{E}-5 & 0 \\ 0 & 0 & 3.5430\text{E}-3 \end{bmatrix} \quad (\text{kg m}^2). \tag{21}$$

One of the matrix elements was verified experimentally, as the experiment was easy to conduct. The experimental result was

$$\text{Experimental result}: \ \bar{I}_{2_{x_2}} = 0.00347 \quad (\text{kg m}^2).$$

The result compared favorably with the calculated value and thus gives us confidence in the remaining analytical results.

The MatLab/Simulink file of model parameters is shown below:

Motor parameters:

```
Kb = 0.0822; %back-emf constant (V-s/rad)
Kt = 0.0833; %torque constant (N-m/A)
R_motor = 1.0435; %resistance (ohms)
L = 3.3E-3; %inductance (H)
B_motor = 0; %viscous damping constant (N-m-s/rad)
Tf_motor = 0.0124; %Coulomb friction (N-m)
J = 4.1E-5; %inertia (kg-m^2)
```

Horizontal Arm parameters:

```
g = 9.81; %m/s^2
Lll = -0.01; %meters
Ll = 0.210; %meters
Ml = 0.911; %kg
l_bar_l_zl = 0.0169; %kg-m^2 mass moment of inertia of arm about
z axis (rotation axis) through its own CG
Tf_theta = 0.0368; %friction torque (N-m)
B_theta = 0; %viscous friction
```

Pendulum parameters:

```
M2 = 0.1326; %kg
L2l = 0.1885; %meters
```

```
I_bar_2_y2 = 0; %actually 2.8457E-5 kg-m^2
I_bar_2_x2 = 3.5374E-3; %kg-m^2
I_bar_2_z2 = 3.5430E-3; %kg-m^2
I_bar_2_x2y2 = -6.538E-5; %kg-m^2
Tf_alpha = 1.8E-4; %N-m
B_alpha = 2.0E-4; %N-m-s/rad
```

3.5. Control system design: balancing and swing-up

A MatLab/Simulink block diagram of the control system design is shown in Figs. 4 and 5. The swing-up control is based on the work of Astrom and Furuta [1] and the balancing controller is a full-state-feedback regulator.

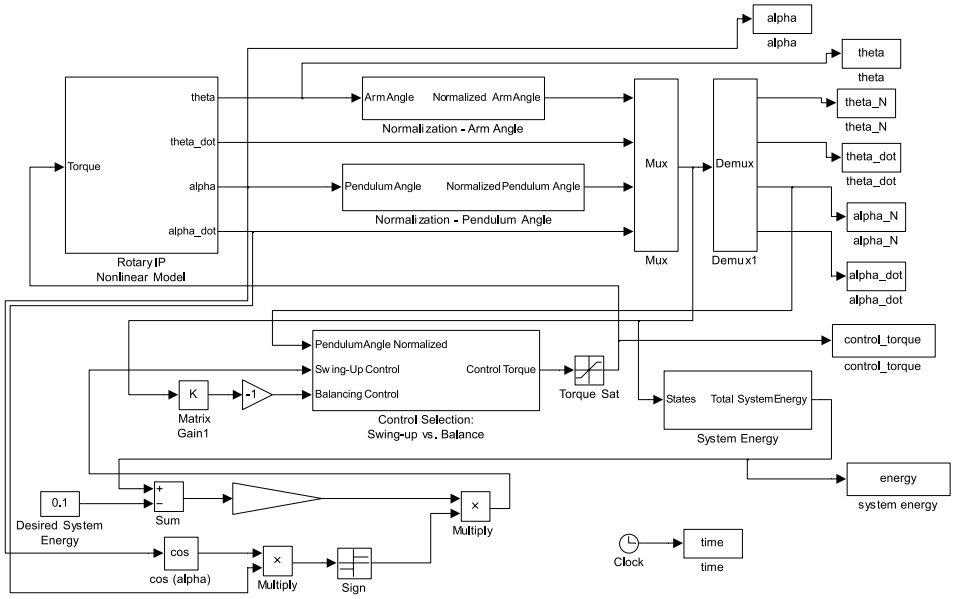

Fig. 4. Matlab/Simulink block diagram of control system design.

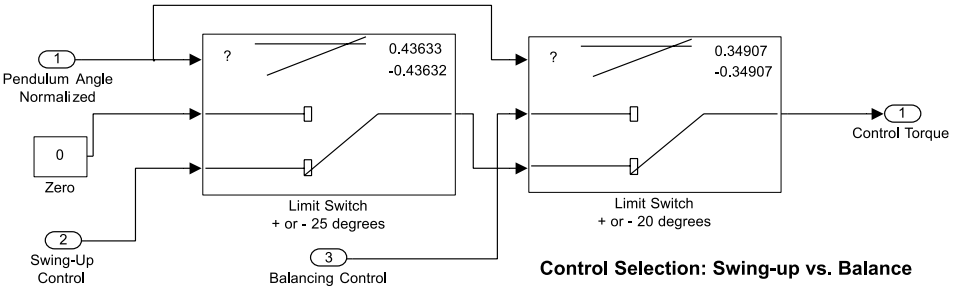

Fig. 5. MatLab/Simulink block diagram of the control-selection subsystem.

The swing-up controller calculates the total system energy based on the kinetic energy of both links, and the potential energy of the pendulum. This calculated value is compared to a defined quantity of energy when the pendulum is balanced. The difference between desired energy and actual energy is multiplied by an "aggressivity" gain and applied to the motor.

To simplify the calculations, the balanced, stationary position of the inverted pendulum is defined to be at zero energy level. The objective of the swing-up control exercise is to move the system from the stable equilibrium position to the unstable equilibrium position. Hence, energy has to be added to the system to achieve this swing-up action. The manipulated input to realize the above idea is given by the following control law:

$$V = K_{\mathrm{A}}(E - E_{\mathrm{O}})\mathrm{sign}(\dot{\alpha}\cos\alpha). \tag{22}$$

The first two terms in the above control law are the aggressivity gain and the difference between actual and desired system energy. These two terms provide the magnitude of energy that has to be added to the system at any given time. The aggressivity gain determines what proportion of the available input will be used to increase or decrease the system energy. This gain could be the difference in swinging the pendulum up in 5 or 50 oscillations.

The second half of the energy swing-up equation determines the direction the input should be applied to increase the energy of the system. The velocity term causes

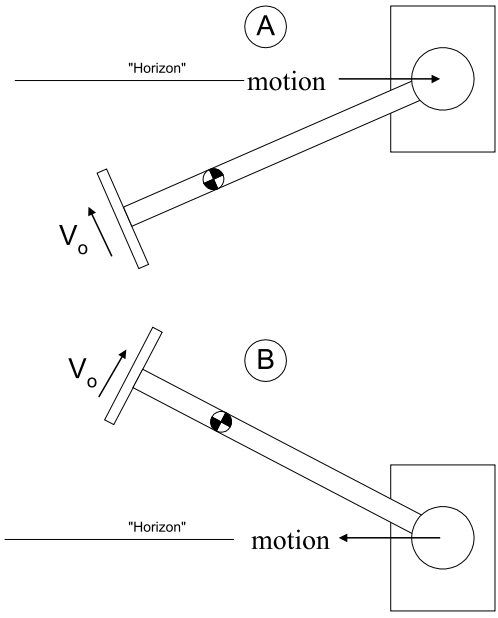

Fig. 6. Sign function effect on swing-up.

the input to change directions when the pendulum stops and begins to swing in the opposite direction. The cosine term is negative when the pendulum is below horizontal and positive above horizontal. This helps the driven link to get under the pendulum and catch it as shown in Fig. 6.

By controlling on energy feedback, the system automatically stops inputting excess energy and allows the system to coast to a balanced position. From Fig. 7, when the remaining potential energy required is equal to the kinetic energy, the feedback will become very small and the pendulum will coast to vertical position.

By setting the desired energy to a value greater than zero, unmodeled energy dissipation effects can be overcome as the pendulum is approaching its balanced point. If this is too much, the pendulum will overshoot and the driven link will not be able to catch it. The switching between the controllers has a dead-band of 5°. When the pendulum is within $\pm 25°$ of vertical, the swing-up controller will turn off. If the pendulum coasts to within $\pm 20°$ of vertical, the balance controller will be activated and the driven link will attempt to catch the pendulum. If the balance controller is not successful, the pendulum will fall and the swing-up algorithm will automatically engage.

Figs. 8 and 9 show the simulation results for the swing-up and balance controllers. The angles plotted are normalized angles.

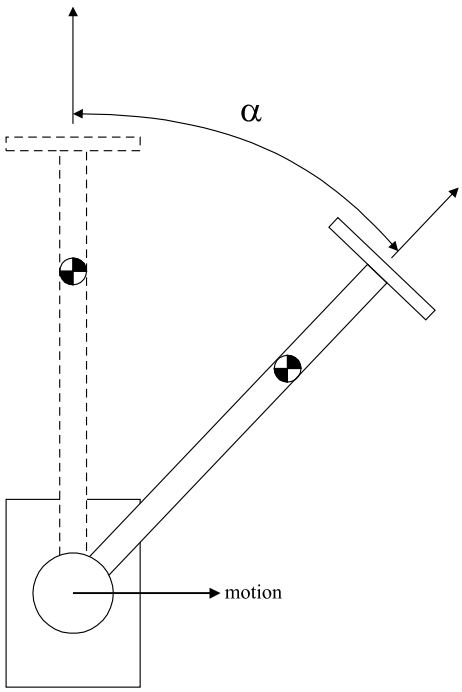

Fig. 7. Swing-up diagram.

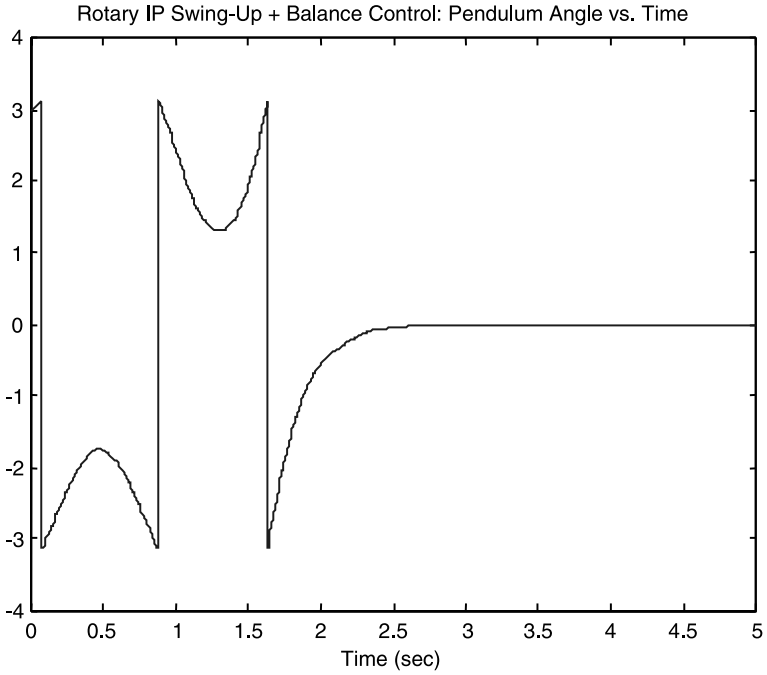

Fig. 8. Normalized pendulum angle versus time.

Fig. 9. Normalized driven link angle versus time.

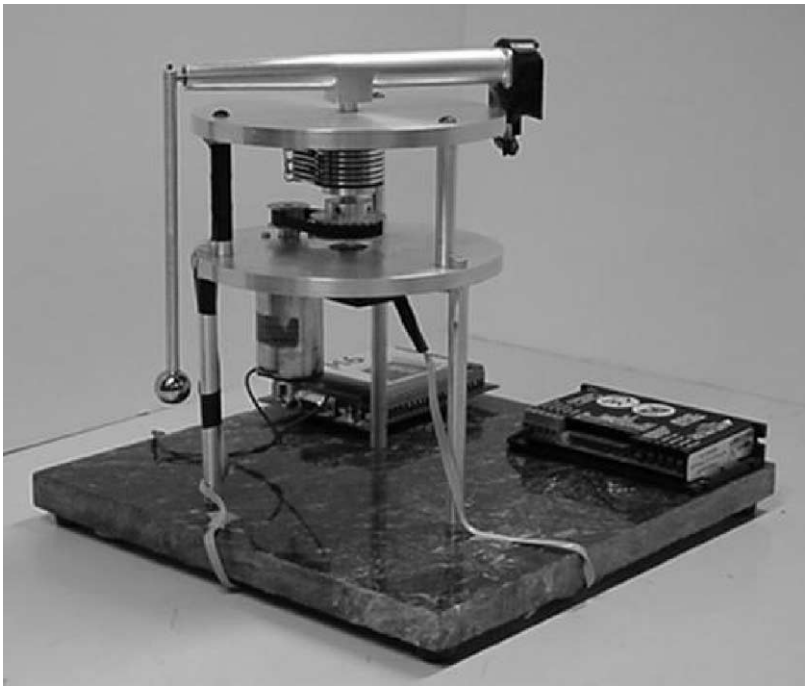

Fig. 10. Small version of the rotary inverted pendulum system.

4. Continuing work

There are two on-going student projects that are continuations of this work:

1. Development of the swing-up and balancing controller for the arm-driven inverted pendulum system.
2. Development of a smaller version of the rotary inverted pendulum system including microcontroller control implementation. The prototype is shown in Fig. 10.

Reference

[1] Astrom KJ, Furuta K. Swinging up a pendulum by energy control. In: IFAC 13th World Congress, San Francisco, CA; 1996.